Microstructural and heat treatment analysis of 316L elaborated by SLM additive manufacturing process

Kaoutar Fri, Abdellah Laazizi, Mouad Bensada, Mohammed El Alami, Abdelmalek Ouannou, Iatimad Akhrif, Mostapha El Jai, Jamal Fajoui

Microstructural and heat treatment analysis of 316L elaborated by SLM additive manufacturing process

Kaoutar Fri[1] · Abdellah Laazizi[1] · Mouad Bensada[1] · Mohammed El Alami[1] · Abdelmalek Ouannou[1] · Iatimad Akhrif[2] · Mostapha El Jai[1,2] · Jamal Fajoui[3]

Metal additive manufacturing is an emerging advanced technology, it differs from conventional manufacturing methods as machining, casting, and forging, which are either subtractive or forming. Firstly, the objective of this work is to elaborate a new 316L stainless steel material by selective laser melting (SLM) from metallic powder according to specific operating parameters, namely laser scanning speed and power. Secondly, the characterization of this developed material by 3D print-ing is carried out. For this purpose, metallographic observations and heat treatments at different temperatures 650, 800, and 1050 °C were performed. Thus, the contribution of this study is to develop procedure and tools to enhance their mechanical properties at the level of parts obtained by conventional processes. Therefore, samples were examined by X-RF, SEM, EDS mapping, density, and hardness measurements as well. The results show that mechanical properties of additive manufactured samples can be improved in certain conditions linked to operating parameters and heat treatment. Also, this work has allowed us to confirm the resistance of the 316L stainless steel developed by SLM to high temperatures.

Keywords 316L stainless steel · Additive manufacturing · Heat treatment · Mechanical properties · Microstructural analysis

Abbreviations

AM	Additive manufacturing
CAD	Computer-aided design
DMLS	Direct metal laser sintering
EDS	Energy-dispersive X-ray spectroscopy
E_D	Deposited energy (J/mm^3)
HV	Vickers hardness
Pi	Laser power (W)
SEM	Scanning electron microscope
SLS	Selective laser sintering
SLM	Selective laser melting
Ti	Heat treating temperature (°C)
Vj	Laser scanning speed (mm/s)
XR-F	X-ray fluorescence spectroscopy
d	Powder bed thickness (50 µm)
h	Hatch space (120 µm)

✉ Abdellah Laazizi
a.laazizi@ensam.umi.ac.ma; abdellah.laazizi@gmail.com

Kaoutar Fri
k.fri@edu.umi.ac.ma

[1] SECNDCM-L2MC, ENSAM-Meknes, Moulay Ismail University, Meknes city, Morocco

[2] Euromed Polytechnic School, Euromed Center of Research, Euromed University of Fez, Fez, Morocco

[3] Ecole Centrale Nantes, Institute of Research in Civil and Mechanical Engineering (UMR CNRS 6183), Saint-Nazaire, University of Nantes, Nantes, France

1 Introduction

Additive manufacturing (AM) has many advantages and will be part of the manufacturing process solutions in a sustainable way. Therefore, it will have a strong impact on manufacturing industry in the near future. Many experts have seen it as an industrial revolution replacing conventional processes and accelerating gains and productivity [1–5]. Actually, a wide range of materials can be used in additive manufacturing processes, including polymer, ceramic, and metallic materials. Steels, titanium (Ti), and Ti-based alloys are widely employed in aeronautics, automobiles, chemicals, and defense, even biomedical because of their high specific resistance, intrinsic value of lightness, sufficient rigidity, mechanical properties, and above all their remarkable resistance to corrosion [6, 7].

Up to now, obtaining high mechanical proprieties and good material integrity are challenging steps. Often, pieces

are subjected to additional posttreatment in order to improve their properties. In order to make selective choices in additive manufacturing, it is necessary to have a good understanding of the existing processes, their constraints and specificities [8, 9]. Three main inputs are required for additive manufacturing: materials, CAD model, and power source or phase transformation tool.

In the case of metallic materials, DMLS or SLS and SLM are the most used processes [10–12]. These technologies cover a variety of processes opposite to the philosophy of subtractive manufacturing where material is removed. In AM, material is joined or solidified under computer control (CAD model) to create a three-dimensional object that meets the desired shape (Fig. 1) and based on the utilized processing parameters, to create parts by SLM. The overall physical properties can be substantially varied considerably relative to the bulk properties of the same conventionally processed alloy [9, 13–16].

The physical and mechanical properties of SLM can be affected by the heating conditions, including rapid cooling (107 °C/s) [13–15], that can be induce to nonequilibrium states which entrap impurities, create residual stress, or produce regions of amorphous material. Non fused powder may exist when it has not properly wetted the metal underneath due to an oxide film or/and treatment power. The porosity is likewise generated by the stripping of the powder and vaporization of the metal [16, 17]. These transformations may have a negative influence on mechanical properties of final manufactured parts.

Simmons et al. [18] showed that, in the case of SLM, thermal profile alters the microstructure compared to conventionally processed materials as well as locally altering the heat conductivity of complementarily constructed 316L stainless steel. When processing conditions use suboptimal densities of energy, the overall the heat conductivities are 10% lower than the estimated theoretical prediction of the average effective thermal conductance.

The influence of different printing orientations and inclinations, with different scan times, on mechanical properties of 17-4PH stainless steel specimens produced by selective laser melting (SLM) have been studied by F.R. Andreacola et al. [19]. They have found that the highest ductility was obtained for the specimen printed horizontally with an inclination of 5° (for both as-built and heat-treated specimens) for the samples treated with scanning times of 50 and 65 s. In addition, according to Wang et al. [20], the amount of applied laser energy has a significant influence on the splash throughout the SLM process. Increased energy results in higher splash intensity, which increase and disperse around the melt and away from the molten pool.

In this paper, the purpose is to characterize additive manufactured materials from the hardness and morphological standpoints for both as-built and heat-treated samples. For this objective, samples are elaborated by using SLM process

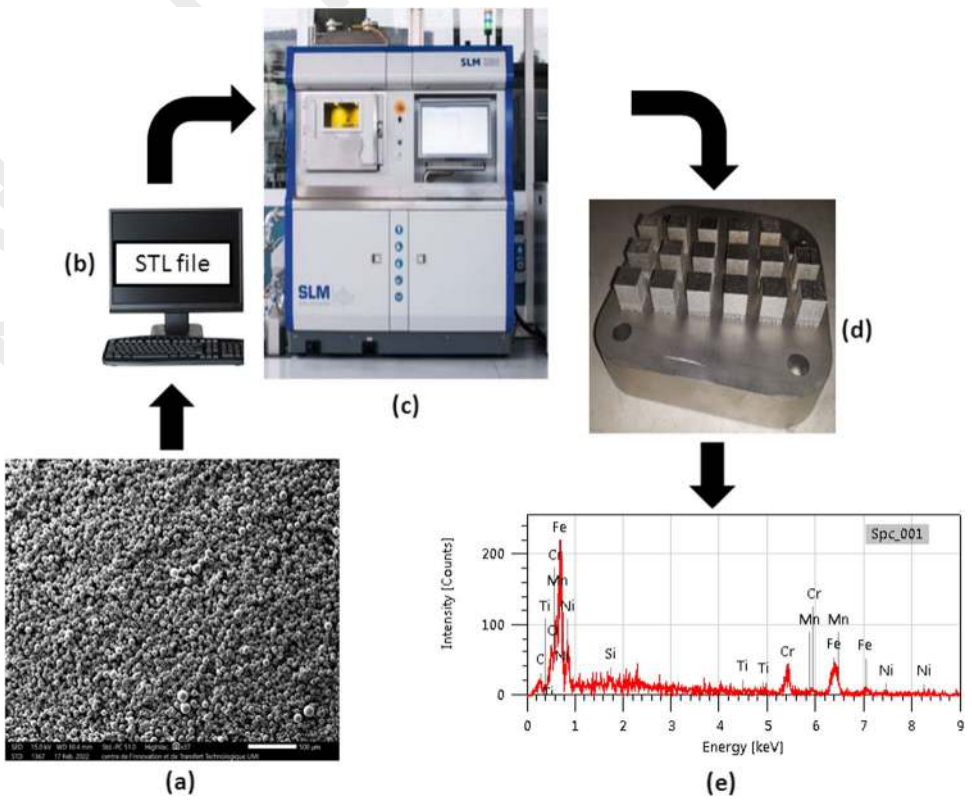

Fig. 1 Additive manufacturing process followed in this study. **a** SEM analysis of powder, **b** parts CAD creation: STL file, **c** used machine SLM 125HL, **d** building samples, **e** chemical analysis by EDS spectrum

with various conditions and examined by XR-F, SEM, EDS mapping, and their density as well. The effect of heat treatment conditions on the hardness of manufactured samples is discussed. SEM and metallographic analysis are employed to verify the developed porosity and the microstructures before and after heat treatment of the produced samples.

2 Selective laser melting (SLM)

2.1 Process and sample preparation

The choice of strategy has a significant impact on the process development and device design; the maturity of these processes has been significantly improved due to the search for new procedure and materials, which have led to robust and stable processes.

SLM is a typically metal powder additive manufacturing process that produces quasi-final forms of parts by the melting and assembly of powder materials in a layer-by-layer model. In this study, for elaborating samples, Nd-YAG laser was used. Once depositing every powder layer, that layer is scanned by the high-power laser. Generated heat by laser melts the powder and fuses it as it cools to a solid metal. The whole operation is repeated to build the pattern layer by layer (Fig. 1). This operation is carried out under the condition of vacuum to avoid the influence of moisture absorption of powders on final forming quality [21].

The main setting parameters that may be controlled include laser power, powder layer thickness; hatch spacing; and laser scan speed. In this work, the thickness of powder layer deposited is 50 μm, and the scanning strategy is Chess.

In this experimental section, samples have been fabricated from 316L stainless steel powder using AM-SLM and tested in both sides: the lateral "FS" and upper "FT" (Fig. 1-e). They were produced using different combinations of operating parameters, namely speed and power of laser. The choice of the parameters was made in accordance with the feature of the machine SLM125HL (Fig. 1-c) and the nature of the material. In order to improve the absorption rate of the laser energy by the metal powder, an Nd-YAG laser with a wavelength of 1064 nm is used. Two scanning speeds V1 = 200 mm/s and V2 = 300 mm/s and three powers P1 = 100 W, P2 = 200 W, and P3 = 300 W have been selected (Table 1).

The second main objective of this survey is the characterization of this new material developed by 3D printing. Therefore, metallurgical studies and mechanical measurements are performed on several samples. Scanning electron microscopy (SEM) analyses were achieved with JEOL JSM-IT500HR equipment and EDS analysis system on steel powders and also on the specimens manufactured by SLM to investigate the surface morphology and the shape of the powder particles. Then, hardness measurements are done with (F = 4.9 N, 15 s).

Table 1 Operating parameters (T0 = 90 °C) of developed samples (as-built)

	As-built (T0 = 90 °C)	
Speed (mm/s) Power (W)	V1	V2
P1	P1V1T0	P1V2T0
P2	P2V1T0	P2V2T0
P3	P3V1T0	P3V2T0

2.2 SEM and X-RF analysis (as-built)

The powder quality and its composition play an important role in the quality of the additive manufacturing processes as it influences not only consolidation phenomena and consequently porosities but also microstructure and final alloy composition. Olakanmi et al. [22] demonstrate that the density of the parts is decreased when the powder particles are heterogeneous in shape. Spherical particles facilitate layer densification because they generate little interparticle friction and have better mobility [23].

The most of the powder particles used in this SLM process have a diameter lower than 50 μm whatever the thickness of the powder bed defined. The size and particle size distribution of the particles have a strong impact on the flow ability of the powder. Smaller particle sizes (diameters less than 15 μm) will tend to form clusters and thus prevent uniform deposition of the powder on the build plate [24].

A mixture of small and large powder particles is preferred for the powder bed melting process, where the small particles percolate through the larger particles to fill the interparticle pores [25] and achieve an optimal powder bed density. The powder particle size has an effect on the final density of the parts produced by SLM. Indeed, Chen et al. [26] analyzed the influence that two differently sized powder batches had on density of final parts with fixed SLM parameters. The batch containing particles of average size lower than 16 μm led to denser parts than the batch with powder of average size 48 μm.

From the SEM image in Fig. 2, it can be seen that most of the powders are spherical; the grains sizes of the powder used in the present work vary from 10 to 50 μm with a centered grain size distribution as it is displayed in Fig. 3. The powder grain size distribution shows a centered behavior distribution. The best fit was assigned to the t-location scale probability function with the following parameters:

- Estimated mean: $\mu = 17.987$ μm
- Estimated standard deviation: $\sigma = 3.065$ μm

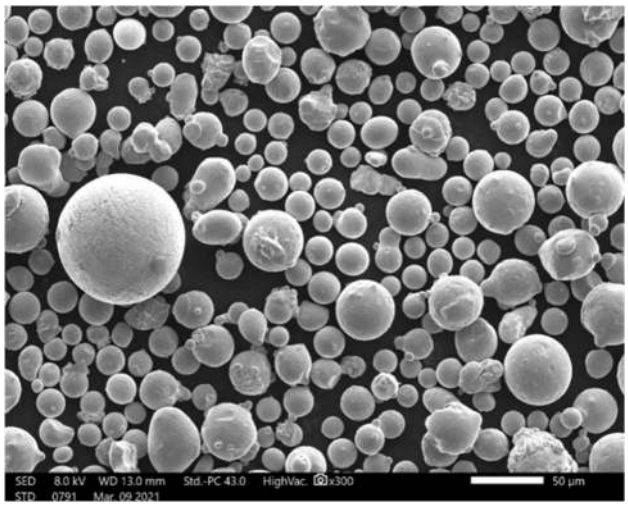

Fig. 2 SEM image of SS 316 L used powder

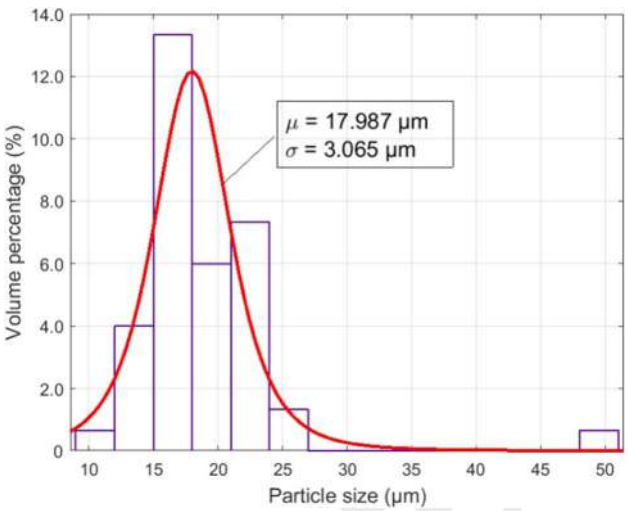

Fig. 3 Powder size distribution with the corresponding fitting

– Estimated shape coefficient: $\nu = 3.688$

The powder was provided from the machine provider SLM Solution Group AG (Lübeck, Germany) to the Euromed University of Fes where the samples were fabricated. The chemical composition of the based material which is 316L powder before SLM manufacturing was examined by X-RF (Table 2) and EDS spectrum (Fig. 4). These results showed that chemical composition has not been affected by AM process.

3 Heat treatment study

It is known that the final obtained microstructure of manufactured parts is correlated to thermal behavior generated within any process. Yet, local heating and fast melting/solidification complicate the control during the multilayer deposition of the SLM process. It is generally through their microstructure and hardness that metals reveal their different mechanical properties. Hardness testing and metallographic observations are therefore essential for any study of materials elaboration. Thus, the impact of heat treatment upon the properties of a stainless steel produced by additive manufacturing is discussed for different operating parameters including power and scanning speed.

3.1 Heat treatment conditions

Heat treatment of metal alloys can be used effectively to achieve the desired mechanical properties of the alloy. Up to now, only a few number of studies have been studied the effect of the heat treatments on SLM 316L properties. Many of occurred phase transformations are controlled by the temperature and duration of the heat treatment. Hardening is one of the heat treatment processes that reinforce and toughen materials such as steel and other irons-based alloys.

Liu et al. [27] showed that the subsequent thermal cycle (STC), being a unique heat behavior within the selective laser melting (SLM) multilayer manufacturing process, has a substantial effect on the thermal behavior within the SLM process and thereby impacts the microstructure of the manufactured components. Also, when the laser beams a layer, the nearby underlying layer can be deeply remelted forming a perfect joint between the neighboring layers, and excellent mechanical properties can be achieved.

Heat treatments are used to improve the properties of the treated material. In this work, samples are classified into three groups according to the treatment they will undergo (T6, T8, and T10). Meanwhile, the temperature and the cooling rate are adjusted, as the holding times are immutable: 10 min (Table 3).

In the first case T6, samples are heated up to 650 °C and submitted to air cooling. In the second case T8, samples are heated up to 800 °C. Then, they are annealed. In the last case

Table 2 Chemical composition of in situ 316L powder measured by X-RF

Element	Si	Cr	Mn	Ni	Sn	Mo	W	Fe
Wt.%	0.25	17.74	1.29	11.69	0.08	2.94	0.04	Bal

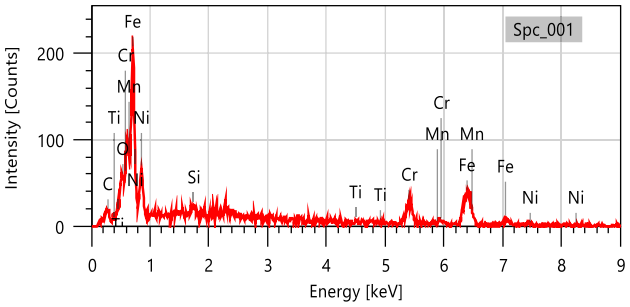

Fig. 4 Chemical analysis by EDS Spectrum of the used powder

(hydrofluoric acid) and observed in samples P3V1T8 and P3V1T10 as it is depicted in Fig. 6. The dendrite arms are assumed to be present when molten metal alloy is cooled instantly or faster for diffusion to take place.

Deposited energy indicates the amount of energy applied per volume of powder material (Table 4). The corresponding deposited energy E_D(J/mm^3) is computed according to the following equation:

$$E_D = \frac{P}{V_i.h.d}$$

where

Table 3 Heat treatment conditions (T6, T8, and T10)

	Air cooling (T6 = 650 °C)		Annealing (T8 = 800 °C)		Hyper quenching (T10 = 1050 °C)	
Speed (mm/s) Power (W)	V1	V2	V1	V2	V1	V2
P1	P1V1T6	P1V2T6	P1V1T8	P1V2T8	P1V1T10	P1V2T10
P2	P2V1T6	P2V2T6	P2V1T8	P2V2T8	P2V1T10	P2V2T10
P3	P3V1T6	P3V2T6	P3V1T8	P3V2T8	P3V1T10	P3V2T10

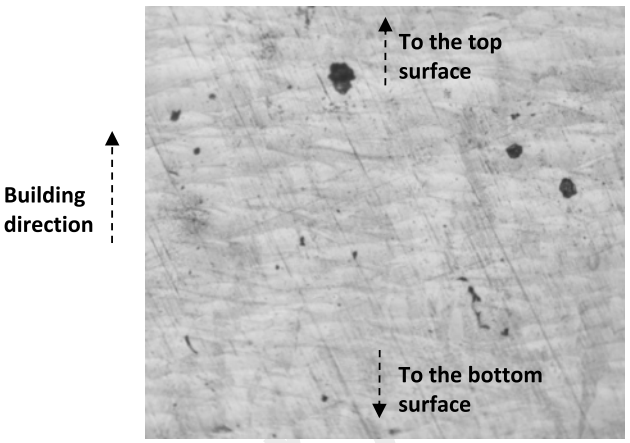

Fig. 5 Typical microstructure obtained for sample on the side surface (FS) without heat treatment

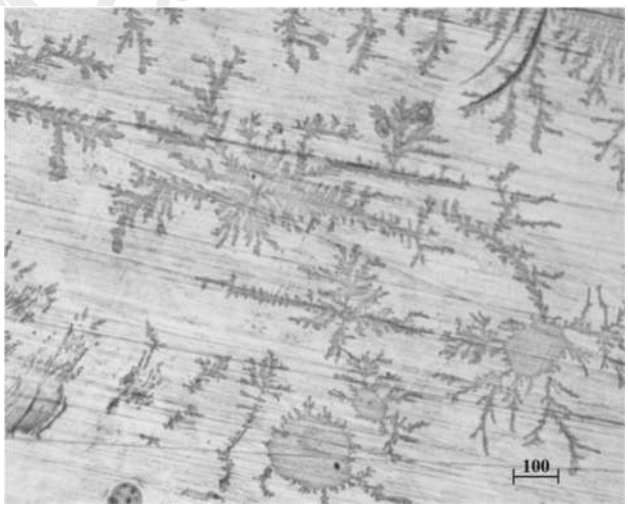

Fig. 6 Microstructure obtained for sample P3V1T10 on the side sur-face (FS) after heat treatment

T10, samples are heated up to 1050 °C and then objected to hyper quenching.

Contrary to conventional stainless steels, the microscopic observations revealed that the transformation of the microstructure of certain samples; for T6 = 650 °C, the microstructures of all samples (P1V1T6, P1V2T6, P2V1T6, P2V2T6, P3V1T6, and P3V2T6) did not significantly change unless elimination of diffusion affected zone and obtaining higher levels of homogeneity across the joint region (Fig. 5). However, dendritic structure on both sides (FS and FT) can be distinguished after typical etching

Table 4 Deposited energy (J/mm^3)

	As-built (T0 = 90 °C)	
Speed (mm/s) Power (W)	V1	V2
P1	83.33	55.55
P2	166.66	111.11
P3	250	166.66

h hatch space (120 µm)

d powder bed thickness (50 µm)

V_i laser scan speed (mm/s)

Moreover, Fig. 5 shows typical microstructure of P3V1 samples with apparent droplets' front's curvatures that resulted from the local melting. These samples were subjected to the high deposited energy in the manufacturing stage, around 250 W as it is depicted in Table 4 for the corresponding cell (P3, V1). In addition, the clearly apparent pores of the same figure can be seen as the result of high flowability of the metal at liquid state which flows in the vertical side according to the gravity.

3.2 Heat treatment effect

In the case of the parts obtained without heat treatment which are designated as-built, Fig. 7 shows that when the laser power increases the hardness also increases for V2 = 300 mm/s. In addition, measured hardness in top side (FT), which is the building direction (z), is different to lateral side (Fs). This result confirmed the results obtained by tensile tests [28]. On the other hand, after the heat treatments, the hardness increases until P2 and decreases at P3 (Fig. 8). To explain these results, deeper analysis especially material densities are carried out.

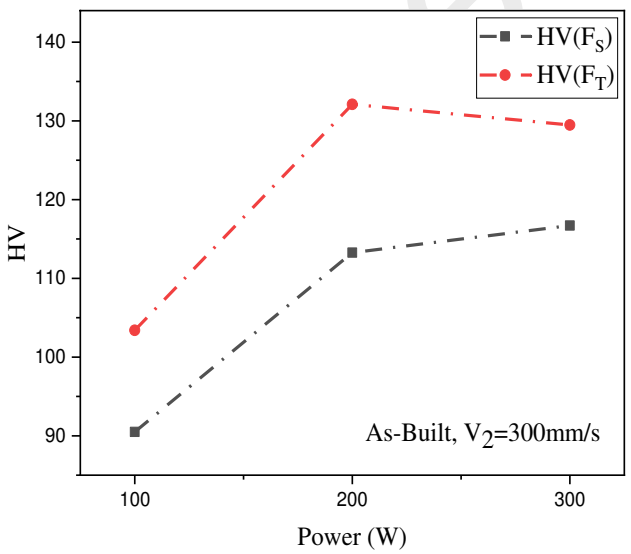

Fig. 7 Hardness values without heat treatment of both sides (upper "T" and lateral "S")

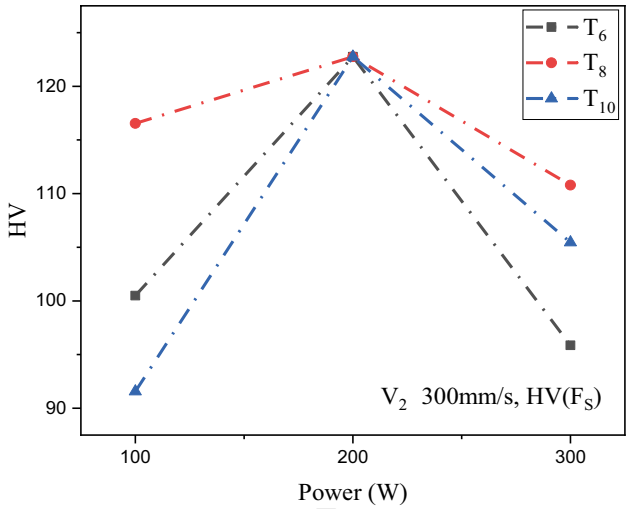

Fig. 8 Hardness values after heat treatment

4 Impact of SLM parameters on material density

Among the objective of selective laser melting fabrication is to obtain a good material with reliable characteristics, directly after fabrication, with respect to mechanical strength, density, material continuity, absence of voids, and surface finish. However, despite the optimization of the density, porosities are inevitable defects that are always found in parts made by SLM if processing parameters are not well determined.

At fixed SLM parameters, powders of different particle sizes will lead to the formation of parts with different densities. However, powders of different particle sizes can be used on the same SLM printer, but the process parameters must be adjusted and optimized for each powder batch [29].

In the study of Spierings et al. [30], three powder batches of different particle sizes (15, 28, and 37 µm) were tested. They obtained parts with higher densities greater than 99% only by adjusting the laser power and scanning speed of the SLM process.

Similarly, Kamath et al. [31] produced 316L steel parts from two batches of powder with different particle sizes. They obtain more than 99% dense parts for both powder batches using laser power above 250 W. The energy deposited was sufficient to fuse all the powder particles and lead to a denser material.

Then, parts made by selective laser fusion on powder bed reach relative densities higher than 99% when all the parameters of the manufacturing chain are optimized [32]. With the same SLM parameters, parts made by SLM from gas atomized powders have better relative density than those consolidated from water atomized powders [33]. Based on these results, gas

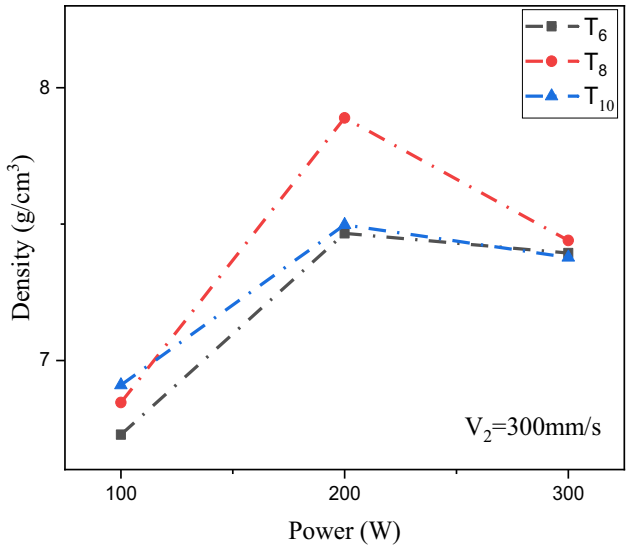

Fig. 9 The density values after heat treatment for V2 = 300 mm/s

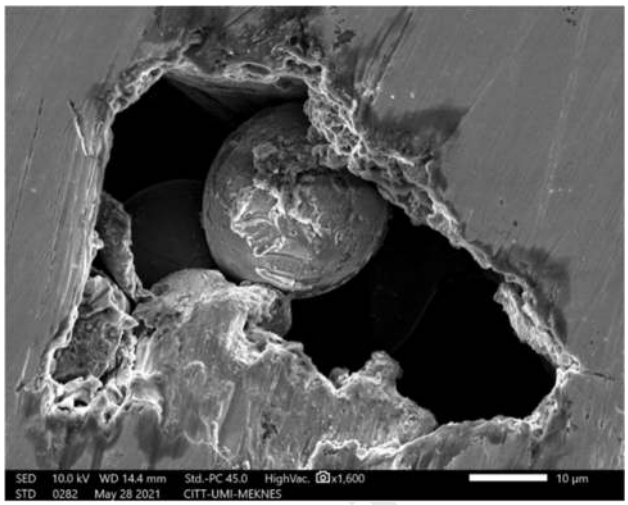

Fig. 10 Cavity observed by SEM of manufactured part P1V1T10 due to non-fusion of grain

atomized powders are widely preferred for the selective laser melting process on powder bed [34].

In this study, density measurements are conducted with Hildebrand Densimeter H-300S. We notice that after heat treatment, the power 200 W is optimal to have an adequate density notably the samples treated with the temperature of 850 °C (Fig. 9). Also, the samples treated and processed with a low scanning speed of 200 mm/s (Fig. 9) are denser than the samples treated with 300 mm/s and this explains the incomplete fusion of the powder and the discontinuity of the material P1V1T10 (Fig. 10).

In the following section, an energy dispersive X-ray spectroscopy (EDS) analysis was also performed thoroughly on the samples, to analyze the distribution of nano precipitates in different micro regions (Fig. 4). Moreover, based on these results (Tables 2 and 5), it can be seen that there is almost no difference between them for main chemical elements if machine uncertainty is taken into account, which confirms the performance of the SLM process in terms of conservation of the initial composition of the powder. Moreover, the reported data shows that the percent of Cr decreased from 17.74 to 17.4 wt.%. This result can be explained by formation of Cr_2O_3 and chromium carbides in surface and grain boundaries during cooling period. These results are confirmed by EDS Spectrum analysis (Fig. 4).

In the case of samples where hardness and densities are low, SEM analysis revealed cavities in bulk materials. These cavities are created due to low laser power and high scanning speed or in case of rapid solidification. The corresponding width seizes are about 70 µm as it was measured from the SEM of Fig. 10. The presence of these defects facilitates cracking path and the premature material failure.

5 Conclusion

Selective laser melting additive manufacturing is a promising technology to produce high-quality shape materials. It is becoming a very suitable process to produce high strength steel. In this paper, the effects of laser scanning speed and power of SLM on the microstructure of the developed material have been studied. The main conclusions drawn from this work are the following:

- Experimental results showed that the effect of power is not always linear after heat treatment. Increasing laser power may lead to low mechanical proprieties.
- Mechanical characterization is carried out mainly the hardness and density and microstructure analyses as well. In the case of heat treatments (650 and 800 °C), the samples did not undergo microstructural changes which confirms the heat resistance of fabricated SLM stainless steels. On the other hand, in the case of T10 (1050 °C), the quenched samples underwent microstructural transformations including the appearance of dendritic structures which explains the change in hardness of the samples.

Table 5 X-RF analysis of material after AM-SLM

Element	Si	Cr	Mn	Ni	Nb	Mo	Ti	Fe
Wt.%	1	17.4	1.2	11.82	0.02	2.68	0.02	Bal

- A microscopic and morphological investigation is conducted by measuring the density of the fabricated material in order to study the effect of the scanning speed on the matter but also on the exterior and apparent sample surfaces. Hence, it was observed that the density shows a drastic drop in the case of high scanning speed such 300 mm/s.
- As long as the hardness of upper side of elaborated samples is higher than lateral side, the elaborated material can be considered as anisotropic. These confirmed results obtained by tensile test. However, the chemical composition of elaborated material by SLM did not change too much compared to initial powder composition.

Acknowledgements The authors greatly acknowledged the help and equipment support from Moulay Ismail University and Euromed Uni-versity of Fez in Morocco.

Author contribution All authors contributed to the study conception and design. Material preparation, data collection, and analysis were performed by all of them. The first draft of the manuscript was written by Kaoutar Fri (PhD student), and all authors commented on previous versions of the manuscript. All authors read and approved the final manuscript.

Declarations

Competing interests The authors declare no competing interests.

References

1. Rivas Santos MV et al (2020) Design and characterisation of an additive manufacturing benchmarking artefact following a design for metrology approach. J Add Manuf 32:100964. https://doi.org/10.1016/j.addma.2019.100964
2. Yap CY et al (2015) Review of selective laser melting: materials and applications. J Appl Phys Rev 2:041101. https://doi.org/10.1063/1.4935926
3. Frazier WE (2014) Metal additive manufacturing: a review. J Mater Eng Perform 23:1917–1928. https://doi.org/10.1007/s11665-014-0958-z
4. Annual Worldwide Progress Report (2013) Additive manufacturing and 3D printing state of the industry, 18th edn. Fort Collins, Wohlers Report
5. El Jai M et al. (2021) Skeleton-based perpendicularly scanning: a new scanning strategy for additive manufacturing, modeling and optimization. Prog Addit Manuf 6:781–820. https://doi.org/10.1007/s40964-021-00197-z
6. Gu D et al (2012) Selective laser melting of TiC/Ti bulk nanocomposites: Influence of nanoscale reinforcement. J Scr Mater 67:185–188. https://doi.org/10.1016/j.scriptamat.2012.04.013
7. Mahamood RM, EAkinlabi T (2017) Laser power and powder flow rate influence on the metallurgy and microhardness of laser metal deposited titanium alloy. J Mater Today Proc 4:3678–3684. https://doi.org/10.1016/j.matpr.2017.02.262
8. He Y et al (2019) Melt pool geometry and microstructure of Ti6Al4V with B additions processed by selective laser melting additive manufacturing. J Mater Des 183:108126. https://doi.org/10.1016/j.matdes.2019.108126
9. Montgomery C et al (2015) "Process mapping of inconel 625 in laser powder bed additive manufacturing", Proceedings Solid Freeform Fabrication Symposium, Austin
10. Harun NH et al (2016) A study on surface roughness during fused Deposition modelling: a review. J Adv Manuf Technol, special issue iDECON. 2289–8107. https://jamt.utem.edu.my/jamt/article/view/3922/2922
11. Sun S, Brandt M, Easton M (2017) Powder bed fusion processes. J Laser Addit Manuf, pp. 55–77. https://doi.org/10.1016/B978-0-08-100433-3.00002-6
12. Patterson AE et al (2019) Experimental design approach for studying Over hanging features in selective laser Melting. J. Adv Manuf Technol 13:2. https://jamt.utem.edu.my/jamt/article/view/5502/3780
13. Pauly S et al. (2018) Experimental determination of cooling rates in selectively laser-melted eutectic Al-33Cu. J Addit Manuf 22:753–757. https://doi.org/10.1016/j.addma.2018.05.034
14. Buchbinder D et al (2011) High power selective laser melting (HP SLM) of aluminum parts. J Phys Procedia 12:271–278. https://doi.org/10.1016/j.phpro.2011.03.035
15. Sun Z et al (2016) Selective laser melting of stainless steel 316L with low porosity and high build rates. J Mater Des 104:197–204. https://doi.org/10.1016/j.matdes.2016.05.035
16. Matthews MJ et al (2016) Denudation of metal powder layers in laser powder bed fusion processes. J Acta Mater 114:33–42. https://doi.org/10.1016/j.actamat.2016.05.017
17. Laazizi A et al (2011) Applied multi-pulsed laser in surface treatment and numerical–experimental analysis. J Opt & Laser Tech 43:1257–1263. https://doi.org/10.1016/j.optlastec.2011.03.019
18. Simmons JC et al (2020) Influence of processing and microstructure on the local and bulk thermal conductivity of selective laser melted 316L stainless steel. J Add Manuf 32:100996. https://doi.org/10.1016/j.addma.2019.100996
19. Andreacola FR et al (2021) Influence of 3D-printing parameters on the mechanical properties of 17–4PH stainless steel produced through selective laser melting. J Frattura ed Integrità Strutturale 58:282–295. https://doi.org/10.3221/IGF-ESIS.58.21
20. Wang D et al (2017) Mechanisms and characteristics of spatter generation in SLM processing and its effect on the properties. J Mat and Desi 117:121–130. https://doi.org/10.1016/j.matdes.2016.12.060
21. Yan X et al (2020) Study of the microstructure and mechanical performance of C-X stainless steel processed by selective laser melting (SLM). J Mat Sci Eng.: A 781:139227. https://doi.org/10.1016/j.msea.2020.139227
22. Olakanmi EO (2013) Selective laser sintering/melting (SLS/SLM) of pure Al, Al–Mg, and Al–Si powders: effect of processing conditions and powder properties. J Mater Process Technol 213:1387–1405. https://doi.org/10.1016/j.jmatprotec.2013.03.009
23. Egger G et al (1999) Optimization of powder layer density in selective laser sintering. Solid Free Fabr Proc. pp. 255–263
24. Weaver JS et al (2021) The effects of particle size distribution on the rheological properties of the powder and the mechanical properties of additively manufactured 17–4 PH stainless steel. J Add Manu 39:101851. https://doi.org/10.1016/j.addma.2021.101851
25. Zhang S et al (2011) Effects of powder characteristics on selective laser melting of 316L stainless steel powder. J Adv Mat Res. pp. 189–193. https://doi.org/10.4028/www.scientific.net/AMR.189-193.3664
26. Chen W et al (2018) Effect of powder feedstock on microstructure and mechanical properties of the 316L stainless steel fabricated by selective laser melting, 8:729. https://doi.org/10.3390/met8090729
27. Liu Y, Zhang J, Pang Z (2018) Numerical and experimental investigation into the subsequent thermal cycling during selective laser

melting of multi-layer 316L stainless steel. J Optics Laser Technol 98. https://doi.org/10.1016/j.optlastec.2017.07.034
28. Wang L (2022) Microstructure and anisotropic tensile performance of 316L stainless steel manufactured by selective laser melting. J Frattura ed Integrità Strutturale 60:380–391. https://doi.org/10.3221/IGF-ESIS.60.26
29. Zhukov A, Deev A, Kuznetsov P (2017) Effect of alloying on the 316L and 321 steels samples obtained by selective laser melting. Phys Procedia 89:172–178. https://doi.org/10.1016/j.phpro.2017.08.010
30. Spierings A, Levy G (2009) Comparison of density of stainless steel 316L parts produced with selective laser melting using different powder grades, 20th Annu. Int Solid Free Fabr Symp SFF
31. Kamath C et al (2014) Density of additively-manufactured, 316L SS parts using laser powder-bed fusion at powers up to 400 W. Int J Adv Manuf Technol 74:65–78. https://doi.org/10.1007/s00170-014-5954-9
32. Vasquez E et al (2019) Elaboration of oxide dispersion strengthened Fe-14Cr stainless steel by selective laser melting. J Mat Pro Tech. 267. https://doi.org/10.1016/j.jmatprotec
33. Cacace S, Demir AG, Semeraro Q (2017) densification mechanism for different types of stainless steel powders in selective laser melting. Procedia CIRP 62:475–480. https://doi.org/10.1016/j.procir.2016.06.010
34. Li R et al (2010) Densification behavior of gas and water atomized 316L stainless steel powder during selective laser melting. J Appl Surf Sci 256:4350–4356. https://doi.org/10.1016/j.apsusc.2010.02.030